



**HAL**  
open science

# Lipid recovery from *Nannochloropsis gaditana* using the wet pathway: Investigation of the operating parameters of bead milling and centrifugal extraction

Vladimir Heredia, Jeremy Pruvost, Olivier Gonçalves, Delphine Drouin, Luc Marchal

## ► To cite this version:

Vladimir Heredia, Jeremy Pruvost, Olivier Gonçalves, Delphine Drouin, Luc Marchal. Lipid recovery from *Nannochloropsis gaditana* using the wet pathway: Investigation of the operating parameters of bead milling and centrifugal extraction. *Algal Research - Biomass, Biofuels and Bioproducts*, 2021, 56, pp.102318. 10.1016/j.algal.2021.102318 . hal-03246073

**HAL Id: hal-03246073**

**<https://hal.inrae.fr/hal-03246073>**

Submitted on 24 May 2023

**HAL** is a multi-disciplinary open access archive for the deposit and dissemination of scientific research documents, whether they are published or not. The documents may come from teaching and research institutions in France or abroad, or from public or private research centers.

L'archive ouverte pluridisciplinaire **HAL**, est destinée au dépôt et à la diffusion de documents scientifiques de niveau recherche, publiés ou non, émanant des établissements d'enseignement et de recherche français ou étrangers, des laboratoires publics ou privés.



Distributed under a Creative Commons Attribution - NonCommercial 4.0 International License

# Lipid recovery from *Nannochloropsis gaditana* using the wet pathway: investigation of the operating parameters of bead milling and centrifugal extraction

Vladimir Heredia<sup>a</sup>, Jeremy Pruvost<sup>a</sup>, Olivier Gonçalves<sup>a</sup>, Delphine Drouin<sup>a</sup>, Luc Marchal<sup>a,\*</sup>

<sup>a</sup> Université de Nantes, Oniris, GEPEA, UMR 6144 F-44600, Saint-Nazaire, France

---

## Abstract

The aim of this work is to track and optimize lipid recovery from *Nannochloropsis gaditana* in wet extraction operations. No significant differences in biomass concentration were found when disrupting microalgal suspensions of up to 30 g/L dry weight, but disruption efficiency differed depending on their physiological states. It took 5.8 minutes in a bead milling device to disrupt 80% of the cells in a nitrogen-depleted culture (10-30 g/L), compared to 4.8 minutes for a nitrogen-replete culture (10-30 g/L). The fatty acids released were then recovered by two different methods: one using a centrifugal partition extractor device and the other using a continuous centrifugal extractor device. For the latter, Box-Behnken RSM analysis showed that the interaction between biomass concentration and solvent inlet rate had the greatest influence on lipid recovery. Up to 84% of the triacylglycerol was recovered using 7.9 g/L of algal suspension at 5.4 mL/min, and treated with 8.9 mL/min of 2-methyl-tetra-hydrofuran.

*Keywords:* Biodiesel, wet extraction, bead milling, centrifugal extraction, experimental design

---

## 1. Introduction

Over the last 20 years or so, biofuels from microalgae, such as biodiesel, have been considered as renewable fuels with which to address the energy crisis, and an option with

---

\*Corresponding author

Email address: [luc.marchal@univ-nantes.fr](mailto:luc.marchal@univ-nantes.fr) (Luc Marchal)

Preprint submitted to Algal Research

April 8, 2021

4 regard to mitigating climate change (CO<sub>2</sub> capture)[1]. The biodiesel production process  
5 involves the production of fatty acids (FAs) by microalgae (which are stored under stress  
6 conditions), the recovery of these energy-rich compounds, and further chemical conversion  
7 of them.

8 There are several microalgae species which can accumulate FAs. The *Nannochloropsis*  
9 genus, in particular, is a diverse collection of microalgae comprising 6 species and several  
10 sub-strains; most of these have been widely studied for biodiesel production due to their  
11 high lipid content under conditions of stress (up to 60%<sub>X</sub>) [2, 3, 4, 5]. *Nannochloropsis*  
12 *gaditana* is one of the most promising strains, producing high levels of lipids [6]. It is  
13 well known that applying stresses such as nitrogen limitation and high light exposure  
14 to microalgae triggers the accumulation of FAs, in particular Triacylglycerol molecules  
15 (TAG) [6, 7, 8]. Stress also seems to affect cell resistance to disruption. It has been  
16 shown that the *Nannochloropsis* genus has a relatively thin cell wall in optimal growing  
17 conditions, but when it is exposed to nitrogen limitation the mechanical resistance of the  
18 cell is somehow increased [2, 9]. This effect could be linked to changes in the cell size or  
19 lipid fraction of the cell wall [10, 11, 12].

20 Although many technologies have been developed for FAs recovery [13, 14, 1, 15, 16],  
21 not all of them can be applied in the biodiesel context, mainly because the processes  
22 used are not always as sustainable, energy-efficient or economically viable as expected.

23 Compared to the energy-intensive operations of the dry pathway, such as biomass  
24 drying and solid-liquid extraction, the wet pathway with its technique of cell disruption  
25 combined with liquid-liquid extraction is a tested option for developing an energy-efficient  
26 process for recovering lipids from microalgae [9, 17, 18, 19, 20]. During cell disruption,  
27 many intracellular components, including FAs, are released into the liquid culture and  
28 can then be recovered using solvents. This dispenses with the drying or dewatering step  
29 involved with the dry pathway and reduces the overall energy required [17, 21, 22, 23].

30 Cell disruption techniques include biochemical methods (*e.g.* enzymes, chemical  
31 treatments, osmotic shock) and mechanical methods (*e.g.* microwaves, ultrasonication,  
32 bead milling, high-pressure homogenization, electroporation) [24, 16]. Mechanical meth-  
33 ods are advantageous because additional reactive compounds, which may degrade or  
34 degenerate beneficial intracellular compounds, are not required. Also, mechanical meth-

35 ods may be less species-specific than biochemical methods, and for some a wider range  
36 of wet biomass concentrations can be treated even for continuous operation. However,  
37 these techniques still need improvement in terms of energy consumption and biomass  
38 concentration efficiency before they can be used in the wet pathway process for biodiesel,  
39 and in terms of understanding and optimizing the undesired effects of some microalgal  
40 intracellular compounds on other downstream processes (*e.g.* liquid-liquid extraction by  
41 solvents)[24, 9, 25, 26, 16, 23].

42 Traditional lipid extraction methods by solvents use a mixture of  $\text{CHCl}_3$  and methanol  
43 [27, 28]. Although non-protic or aprotic polar solvents like hexane and  $\text{CHCl}_3$  [29] have  
44 high lipid-extraction yields, their use at industrial scale would exacerbate environmen-  
45 tal and health problems [30]. Aprotic solvents like ethyl acetate and 2-methyl-tetra-  
46 hydrofuran are an alternative; these are also known as green solvents because they are  
47 produced from renewable raw materials. 2-methyl-tetra-hydrofuran, heptane and 8 oth-  
48 ers have been screened previously for their efficiency in short-time wet extraction. 2-  
49 methyl-tetra-hydrofuran in particular minimizes the energy needed for solvent recycling  
50 and presents low solubility in water [9].

51 Liquid-liquid (L-L) extraction is a method widely used for separating a solute from one  
52 liquid (*i.e.* microalgal culture feed) into another with a relative preference for the solute  
53 (*i.e.* solvent). Efficiency depends mainly on the distribution coefficient of the L-L sys-  
54 tem (and therefore the choice of solvent), the surface and time of contact between phases  
55 (related to mixing), the concentration of the solute (*i.e.* lipid availability) and operat-  
56 ing parameters such as temperature and rate of solvent/feed. At industrial scale, these  
57 parameters can be modulated in mixers/reactors (batch operation) or mixer-settlers and  
58 columns (continuous operation). However, this equipment often requires an additional  
59 separation operation (large separatory funnel or industrial centrifugation/decantation).  
60 In this regard, an approach employing intensified operations would integrate these tech-  
61 nologies and eventually lead to smaller, more energy-efficient process equipment [31, 32].

62 One way of intensifying wet extraction is to use processes based on centrifugal force,  
63 for improved mixing and separation. Systems like continuous centrifugal extraction  
64 (CCE) (Fig. 1a) are designed for continuous L-L extraction and simultaneous sepa-  
65 ration of the phases [33]. CCE mixes two input streams - solvent and algal culture feed

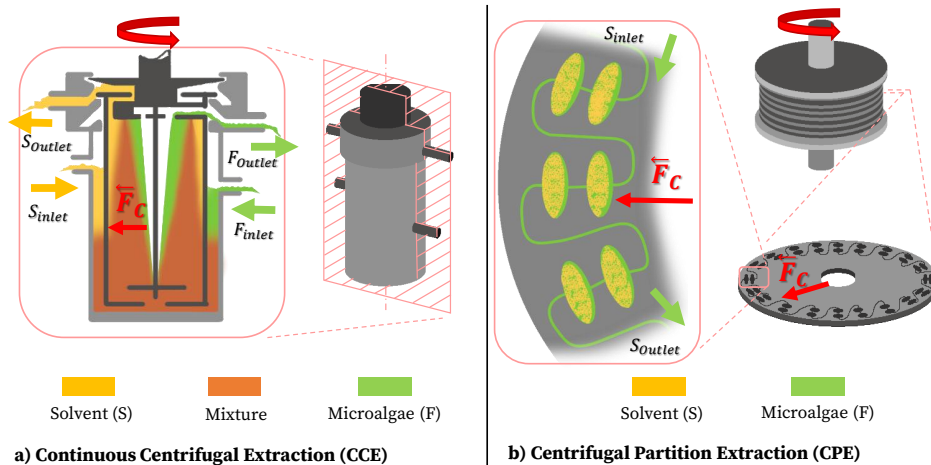


Figure 1: Continuous Centrifugal Extraction and Centrifugal Partition Extraction comparison diagrams.  $F_C$  is the centrifugal force vector.

66 (rich in lipids) - in a common rotary chamber, the speed of which can be modulated.  
 67 Under the right conditions, two separate outlet flows are recovered during extraction: the  
 68 raffinate fraction - which is mostly lean culture, and the extract fraction, which is mostly  
 69 solvent. This equipment is promising for reducing solvent consumption and simplifying  
 70 scale-up of the wet-extraction process due to its adjustable flow-rate capacity and the  
 71 ability to connect several modules in series. However, there are no reports on the use of  
 72 CCE for purely biotechnological applications or biofuel production [34, 32].

73 Another interesting approach for wet-extraction is to use a centrifugal partition ex-  
 74 traction (CPE) device (Fig. 1b). These devices have been widely used for separation  
 75 and recovery purposes in the biotechnology and nutrition industries [33]. The principle  
 76 is similar to L-L chromatography but with no solid support to retain the solutes; it is  
 77 based on the partition coefficient between two non-miscible solvents. CPE devices such  
 78 as, centrifugal partition chromatography (CPC) have a series of small chambers filled  
 79 with solvent as a stationary phase. The stationary phase inside is maintained by apply-  
 80 ing a centrifugal force to the entire series of chambers. A mobile phase is then pumped  
 81 into the system, enabling interaction with the solvent. This way, the solvent elutes the  
 82 solutes every time it enters the chambers. With this technology, the amount of solvent  
 83 used and the operating time are considerably reduced compared to conventional extrac-

84 tion processes, including CCE [35]. For this reason, CPE is a useful comparison point  
85 for efficiency.

86 Some parameters still need to be adjusted for scaling up centrifugal lipid extraction  
87 for biodiesel production. These include: 1) the availability of lipids for the extraction  
88 (lipid concentration function and percentage of disrupted biomass); 2) the establishment  
89 of an adequate solvent/feed ratio for optimal mass transfer; 3) the absence of emulsion  
90 (regularly promoted by the release of intracellular proteins and pH changes after cell  
91 disruption).

92 Analyzing the role of the above parameters in isolation in the extraction process would  
93 be inefficient in terms of time, resources and unknown related interactions. One strategy  
94 for analyzing and optimizing the multiple factors that interact in the phenomenon is  
95 the response surface methodology (RSM). However, prior to running an RSM, a few  
96 exploratory experiments are required to ascertain the trends of the variables.

97 The aim of this work is therefore to enhance lipid recovery from *Nannochloropsis*  
98 *gaditana* by first maximizing lipid availability via bead milling, then optimizing the  
99 main parameters using CCE technology. The optimal lipid recovery obtained is then  
100 compared with a reference CPE and the resulting operational problems discussed in  
101 terms of biodiesel application.

## 102 2. Materials and Methods

### 103 2.1. Microalgal Cultures

104 The microalga *Nannochloropsis gaditana* CCMP527 (NCMA, USA) was grown in  
105 artificial sea water (ASW) [36] enriched with CONWAY solution as the culture medium.  
106 ASW is prepared using (mM): NaCl, 248; Na<sub>2</sub>SO<sub>4</sub>, 17.1; KCl, 5.49; H<sub>3</sub>BO<sub>3</sub>, 0.259;  
107 NaF, 0.045; MgCl<sub>2</sub>-6H<sub>2</sub>O, 32.24; CaCl<sub>2</sub>-2H<sub>2</sub>O, 0.626; KBr, 0.497; SrCl<sub>2</sub>-6H<sub>2</sub>O, 0.056;  
108 NaHCO<sub>3</sub>, 1.42. CONWAY solution uses NaNO<sub>3</sub> as the source of nitrogen, at 10.6 mM.  
109 However, for the experiments referred to as N-replete (optimal conditions), the amount of  
110 NO<sub>3</sub> was doubled to 21.2 mM to ensure there was no nitrogen limitation. For the cultures  
111 referred to as N-depleted (starved conditions), a CONWAY solution was prepared without  
112 NO<sub>3</sub>, and this was added in the same quantity as for the replete culture. All cultures

113 were inoculated with a 10% inoculum/medium ratio using a pre-culture in exponential  
114 cell growth.

115 Three photobioreactors (PBRs) were used to supply enough biomass for the work. For  
116 the early experiments related to cell disruption optimization and solvent choice, two were  
117 set outdoors in France in late summer 2018 (47°15'06.5" N, 2°15'34.5" W) in 170-litre  
118 flat-panel airlift PBRs (Subitec, Germany). These reactors were operated in batch mode  
119 with the pH regulated at 8 by manual injection of 98% CO<sub>2</sub> (gas). For the experiments  
120 related to Box-Behnken RSM, a single 170-litre flat-panel airlift PBR (HECtor PBR)  
121 was operated indoors in batch mode. A description of the reactor is given by Pruvost  
122 et al. [37]. This reactor was irradiated with artificial LED light, simulating the average  
123 annual irradiation (photon flux density 269  $\mu\text{mol}/\text{m}^2\cdot\text{s}$ ) and solar cycles of the above  
124 outdoor conditions. The pH was also set at 8 by automatic CO<sub>2</sub> (gas) injection.

125 The biomass from the depleted and replete cultures was harvested using a continuous  
126 centrifuge (DRA320VX Rousselet Robatel, France) at 6000 rpm (8064 rcf). The sludge  
127 (biomass concentration 40 g/L) was then diluted using a phosphate buffer saline (PBS)  
128 solution to obtain 1, 5, 10, 20 and 30 g/L for cell disruption optimization, and 2, 5 and  
129 10 g/L for the RSM. Note that in addition to the biomass concentration usually obtained  
130 directly from the culture system (1-5 g/L), the range of biomass concentrations in this  
131 case was increased to 30 g/L to simulate the possible use of other pre-concentration  
132 processes for potential medium recycling (such as dissolved air flotation).

## 133 2.2. Dry Weight Analysis

134 Glass fiber filters with a pore diameter of 0.45  $\mu\text{m}$  (Whatman GF/F) were pre-  
135 weighed. 10 mL samples were taken from the PBRs and filtered in triplicate. The  
136 filtered biomass was then washed with 3 equal volumes of NH<sub>4</sub>HCO<sub>2</sub> 1.19 M and 3 equal  
137 volumes of MiliQ water to remove culture medium salts. The filters were dried at 103  
138 °C for 1 hour (no further time needed to achieve weight stabilization) and then weighed.  
139 The biomass concentration (represented by  $X$ ) was considered as the weight difference  
140 between the dry biomass and the empty filters for each culture volume. The values  
141 reported correspond to the mean values in a triplicate dry weight assay.

142 *2.3. Bead Milling*

143 To carry out cell disruption, a continuous bead mill was used in the laboratory  
144 (DYNO-Mill KD, Multilab, WAB, Switzerland). The grinding chamber ( $\approx 0.561$  L)  
145 connected to an agitator disc (64 mm diameter) was filled to 80% with 0.5 mm diameter  
146 glass grinding beads. During the process, milling was carried out at an impeller tip speed  
147 of 14 m/s and a flow biomass inlet rate of 9 L/h, with reference to Zinkoné et al. [25].

148 Three dilutions (10, 20, 30 g/L) for each N-depleted and N-replete outdoor culture  
149 were passed through the bead milling device between 1 and 5 times. The corresponding  
150 aliquot was analyzed after each time to determine the associated disruption rate.

151 *2.4. Quantification of Cell Disruption*

152 The cells were counted digitally using image analysis and a Malassez cell-counting  
153 chamber under microscope. First, a diluted sample was prepared to avoid saturating the  
154 number of cells per image, but enough to provide a representative aliquot of the culture  
155 [25]. Then a Malassez double chamber was prepared and focused at 40x using an optical  
156 microscope connected to a camera (Axio MRC Cam at Axio Scope A1 microscope, Carl  
157 Zeiss, Germany). The camera took 40 pictures of each sample, which were then analyzed  
158 using image-analysis software (ImageJ v.1.52o, NIH, USA) to distinguish images-like-  
159 noise and images-like-cells. The cell surface was calculated in  $\mu m^2$  for all images-like-cells,  
160 based on the distance-to-pixel ratio.

161 This method identified the cell size, shape and surface distribution of the original  
162 culture and compared it to the corresponding values after cell disruption enabling cell  
163 debris to be distinguished from undisrupted cells. The cell count and statistical informa-  
164 tion were then gathered using a MATLAB algorithm (Math-Works, US). Prior to using  
165 this method, it was validated with direct microscope counting (data not shown).

166 The microalgal cell disruption rate  $\tau_D$  was defined as the complementary fraction of  
167 the ratio of cells counted after bead milling to those counted before the process.

168 *2.5. Total Fatty Acid (TFA) and Triacylglycerol (TAG) Extraction Efficiency and Quan-*  
169 *tification*

170 To measure the TFA content, the organic fractions from extraction experiments were  
171 recovered and the corresponding solvent evaporated. The following analysis protocol is



172 adapted from Moutel et al. [38]. An internal standard solution of a known C17:0 fatty  
173 acid concentration and  $\text{CHCl}_3/\text{MeOH}$  was added to corroborate the subsequent findings.

174 To summarize, the sample was derivatized using  $\text{BF}_3$  (catalyst) and MeOH at  $96^\circ\text{C}$   
175 for 10 minutes (VWR International, US). Following the reaction, the sample was washed  
176 using distilled water saturated in hexane to remove catalyst residues. The organic phase  
177 was then recovered and measured by gas chromatography using a flame ionization de-  
178 tector (GC-FID, Agilent Technologies, USA). Fatty acid methyl esters (FAMES) were  
179 determined by comparing their retention time with those of the standards ones used for  
180 calibration. The concentration of each FAME was calculated with Chemstation software  
181 (Agilent Technologies, USA), using C17:0 fatty acid as the internal standard.

182 TAG content was determined by taking an aliquot of the organic fractions from the  
183 extraction experiment and processing it by HPTLC (CAMAG, Switzerland). Samples  
184 between 1 and 20  $\mu\text{L}$  were placed on silica gel plates (20 x 10 cm; Merck Group, Germany)  
185 by auto-sampler. A self-designed mix of polar and non-polar lipids (Sigma-Aldrich, US)  
186 was also placed on the plate as the standard. After sample migration, the plate was  
187 revealed in a chromatogram immersion device with a TLC plate heater, using an ortho-  
188 phosphoric acid and copper sulphate solution. Data acquisition was by TLC Scanner 3  
189 (VisionCats, CAMAG, Switzerland) and related software.

The results for TFA or TAG per gram of algal biomass treated are shown as  $\text{TFA}\%_X$   
or  $\text{TAG}\%_X$ . The extraction efficiency is represented by:

$$\eta_{E,i} = (i_j)/(i_{\text{CHCl}_3/\text{MeOH}}) \quad (1)$$

190 where  $i$  is either  $\text{TFA}\%_X$  or  $\text{TAG}\%_X$  extraction carried out with a specific solvent,  $j$ .

### 191 2.6. Choice of Solvent and Standard Extractions

192 To find out either the TFA or TAG content,  $\text{CHCl}_3/\text{Methanol}$  2:1 v/v (Fisher Sci,  
193 US) was used as a reference solvent for extractions. Other solvents used for comparison  
194 assays were heptane, Hep (Emsure-Merck, Germany), ethyl acetate, EtoAc (Fisher Sci,  
195 US) and 2-methyl-tetra-hydrofuran, Me-THF (Acros Organics-Thermo Fisher Sci, US).  
196 Their main properties are summarized in Table 1.

197 Samples from the depleted cultures were passed through a high-pressure homogenizer  
198 (Constant Systems Ltd, UK) three times at 2.7 Kbar and  $10^\circ\text{C}$ . Passing the samples

Table 1: Main physicochemical properties of heptane (Hep), ethyl acetate (EtoAc) and 2-methyl-tetrahydrofuran (Me-THF)

	Hep	EtoAc	Me-THF
<i>Molecular Formula</i>	C <sub>7</sub> H <sub>16</sub>	C <sub>4</sub> H <sub>8</sub> O <sub>2</sub>	C <sub>5</sub> H <sub>10</sub> O
<i>Density at 20° C - <math>\rho_S</math> (g/mL)</i>	0.684	0.902	0.854
<i>Vapor pressure at 20° C (mmHg)</i>	34.5	73	102
<i>Boiling temperature at <math>P_{atm}</math> (° C)</i>	98.4	77.1	80.2
<i>Viscosity at 25° C (cP)</i>	0.376	0.423	0.46
<i>Solubility in water at 20° C (wt%)</i>	2.2 (25° C)	8.7	14.1
<i>Reference</i>	[39]	[39]	[40]

199 through the equipment three times ensured total destruction of the cells, which was  
 200 verified by microscope observation. The suspension was mixed with the respective solvent  
 201 at 1:2 v/v (solvent per aqueous phase) for 4 hours at 23 °C, the organic phase was then  
 202 recovered and the TFA and TAG concentration determined for the solvents tested.

### 203 2.7. Continuous Centrifugal Extraction

204 The extraction system used was a mono-stage continuous centrifugal extraction (CCE)  
 205 device - type BXP 012 (Rousselet Robatel, France) using N-depleted biomass from the  
 206 HECtor PBR. Biomass concentration was adjusted to the target values (2,5,10 g/L) and  
 207 then disrupted in the bead mill to obtain a cell disruption rate  $\tau_D$  of more than 90%  
 208 (verified by microscope observation). This suspension was considered as the inlet feed.

209 The rotation speed of the CCE device was set beforehand at between 2000 and 4000  
 210 rpm (107-430 rcf) depending on the experiment run. After approximately 20 seconds, the  
 211 speed was stable and the solvent and feed inlet rates ( $S$  and  $F$ ) were set at the established  
 212 flow rate into the system. After an additional 30 - 60 seconds, the extract and raffinate  
 213 fractions ( $E$  and  $R$ ) began to flow out normally and were recovered at the same inlet flow  
 214 rate, which also enabled verification of the total flow supplied ( $ToT = S + F = E + R$ ).  
 215 Around 30 mL from each outlet current (E and R) was then collected and analyzed  
 216 identically by GC-FID and HPTLC to obtain the TFA/TAG extraction efficiency  $\eta_{E,i}$   
 217 for the experiment run.

218 *2.8. Experimental Design for Continuous Centrifugal Extraction*

219 A Box-Benhken experiment was designed using the data collected from the bead  
220 milling optimization and the more efficient solvent. The CCE variables chosen for Box-  
221 Benhken RSM optimization were biomass concentration (after harvesting), solvent inlet  
222 rate and feed inlet rate. For detailed information on the design of the Box-Benhken and  
223 related data processing, see Appendix A.

224 All the experiment runs were immediately batched-executed at 25°C within the first  
225 30 minutes of bead milling, to avoid undesirable reactions due to interaction between the  
226 medium ions and the cell cytoplasm. Samples from each observation unit were stored at  
227 -80°C for determination of further TFA/TAG extraction efficiency ( $\eta_{E,i}$ ).

228 Where emulsification was unavoidable, samples were still taken but centrifuged at  
229 6000 rpm (4226 rcf) and 4°C for 10 minutes (Hettich, Germany), to separate the phases  
230 from the two outlets. The organic phase was then analyzed by the same methods as  
231 described above.

Using the data obtained according to the experimental design, the specific solvent  
consumption  $\Gamma_j$  was calculated as follows:

$$\Gamma_j = (S \cdot \rho_j) / (F \cdot X \cdot \eta_{E,i}) \quad (2)$$

232 where  $S$  is the solvent inlet rate and  $F$  the feed inlet rate (both in mL/min);  $\rho_j$  is the  
233 solvent density in g/mL,  $X$  is the biomass concentration in the feed in g/mL and  $\eta_{E,i}$  is  
234 the extraction efficiency. In this work,  $\Gamma_j$  was only calculated for the optimized condition  
235 in the CCE and analysis of the comparison with the CPE.

236 *2.9. Centrifugal Partition Extraction*

237 Centrifugal partition extraction (CPE) was carried out for comparison with the final  
238 CCE optimization value. Two liters of N-depleted culture at 5 g/L biomass concentration  
239  $X$  were passed through the bead mill several times to obtain a cell disruption rate  $\tau_D$  of  
240 more than 90% (verified by microscope observation). This suspension was treated with  
241 CPE.

242 The CPE device (Model A, Kromaton, France) was fitted with a short column (231  
243 chambers) to carry out TAG extraction with Me-THF. The equipment was set for 1 stage

Table 2: Culture conditions after batch operations. X is biomass concentration, TFA total fatty acid content and TAG triacylglycerol content.

Culture system		X (g/L)	SE (n = 3)	TFA content (% <sub>X</sub> )	TAG content (% <sub>X</sub> )	Index 480/662 nm
Outdoor	N-Replete	2.29	2.29	8.7	2.2	0.51
Outdoor	N-Depleted	0.54	0.02	28.1	13.4	1.83
Indoor	N-Depleted	1.52	0.01	32.2	28.6	3.34

244 at 900 rpm (59 rcf, [41]) in non-continuous mode for a column volume of 270 mL and  
 245 a solvent volume of 140 mL. The disrupted culture suspension was then passed through  
 246 the system at 25 mL/min, allowing 5 minutes for the extraction (residence time). The  
 247 solvent and feed volumes and rates were based on Marchal et al. [42] and Ungureanu  
 248 et al. [35]. The extracted fraction was recovered and analyzed for TAG content and  
 249 consequently TAG extraction efficiency ( $\eta_{E,TAG}$ ).

### 250 3. Results and Discussion

#### 251 3.1. Final Culture Conditions

252 Table 2 shows a summary of the final conditions of the cultures used to produce the  
 253 biomass. After 11 days, the final biomass concentrations for N-depleted and N-replete  
 254 outdoor cultures were 0.54 and 2.29 g/L (SE = 0.02 and 2.29; n = 3) respectively,  
 255 with 28.1%<sub>X</sub> and 8.7%<sub>X</sub> of TFA and 13.4%<sub>X</sub> and 2.2%<sub>X</sub> of TAG respectively. The  
 256 absorbance 480/662 nm index was measured [43] as a reference to compare stress levels  
 257 between the PBRs. The N-depleted and N-replete values on the final day were 1.83  
 258 and 0.51 respectively, indicating that the carotenoids-to-chlorophyll ratio had a strong  
 259 influence on the N-depleted culture and confirming cell stress compared to the N-replete  
 260 culture, as expected.

261 The indoor PBR culture was ended after 13 days. The final biomass concentration  
 262 was 1.52 g/L (SE = 0.01; n = 3) with 32.2%<sub>X</sub> TFA and 28.6%<sub>X</sub> TAG. The 480/662 nm  
 263 index was 3.34 at the end of the culture, which also corroborates the cell stress.

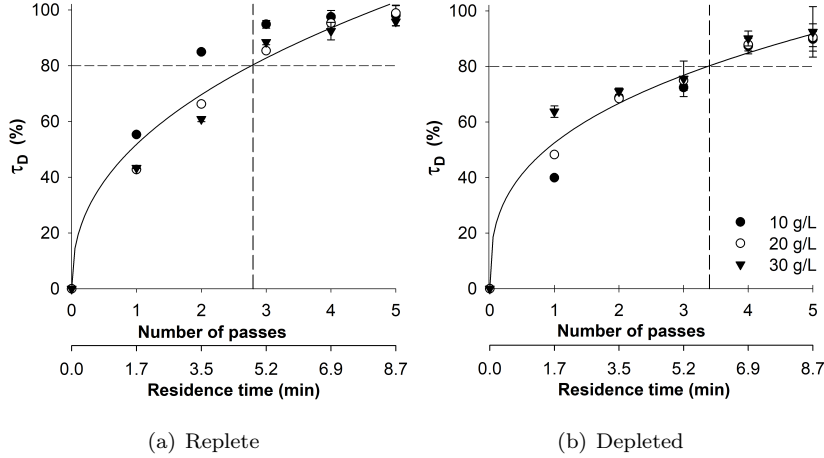


Figure 2: Disruption kinetics at bead milling for N-replete and N-depleted cultures. The disruption rate  $\tau_D$  is plotted for each biomass concentration condition  $X$ , and the two-parameter power regression for each physiological state. Error bars for CI ( $n \approx 20$ ,  $\alpha = 0.05$ )

### 264 3.2. Cell Disruption Optimization

265 Fig. 2 plots the cell disruption rate as a function of the physiological state (as a conse-  
 266 quence of cells adapting to the culture medium) and biomass concentration, throughout  
 267 the operating period. Three different biomass concentrations from two different medium  
 268 conditions (replete and depleted) were processed in a bead mill to find the residence time  
 269 required (*i.e.* number of passes) to achieve a cell disruption rate of 80%. A one-way anal-  
 270 ysis of the variance applied to the disruption rate results from the biomass concentration  
 271 groups at each physiological state revealed that there were no statistically-significant  
 272 differences between the groups (replete:  $F(2, 12) = 0.31$ ,  $p = 0.74$ ; depleted:  $F(2, 12)$   
 273  $= 0.22$ ,  $p = 0.81$ ). Based on this consideration, the whole data set for each physiological  
 274 state was arranged in a two-parameter power regression, as shown in Fig. 2 ( $R^2 = 0.9619$   
 275 for replete,  $R^2 = 0.9776$  for depleted), and the regression equation enabled calculation  
 276 of the exact residence time needed for bead milling to disrupt 80% of the cells: 4.8 min-  
 277 utes for replete culture and 5.8 minutes for depleted culture (both for concentrations of  
 278 between 10 and 30 g/L). The difference is more evident in Fig. 2 where  $\tau_D > 80\%$ . A  
 279 minimum of three passes are required for the replete culture (Fig. 2a) and four passes  
 280 for the depleted culture (Fig. 2b). A comparison of the  $\tau_D$  from different physiological

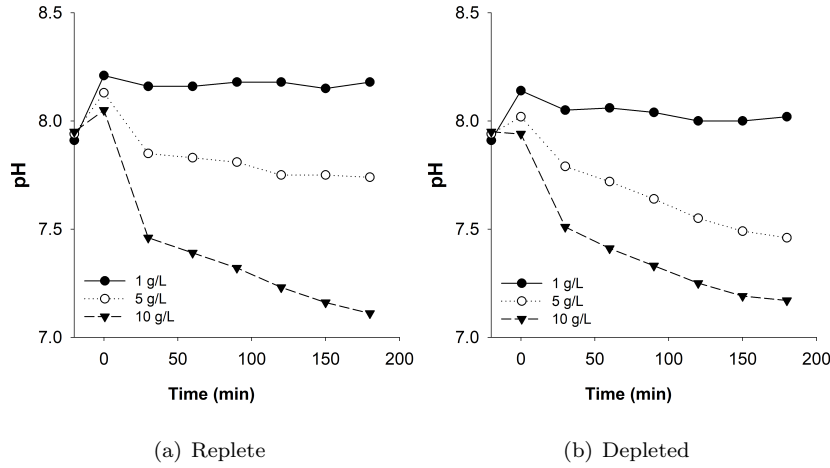


Figure 3: pH value of microalga suspension after passing 4 times through a bead mill for N-replete (a) and N-depleted (b) cultures. For each graph, the value on the left represents the pH before milling; the value at zero represents the moment immediately after milling ( $n = 1$ ).

281 states shows that *N. gaditana* presents more mechanical resistance to milling when it  
 282 is harvested in nitrogen-depleted conditions. A similar result using *Nannochloropsis sp.*  
 283 was obtained by Angles et al. [9].

284 The final pH value after bead milling is important to preserve the integrity of the  
 285 molecules to be recovered, and also the workability of the suspension for further steps,  
 286 mainly emulsification of the lipids and proteins released during the process. For this  
 287 reason, the pH was monitored for biomass concentrations 1, 5 and 10 g/L and for the  
 288 two physiological conditions, after cell destruction. The initial pH was 7.9 for each, as  
 289 shown in Fig. 3. The 10 g/L suspensions for both physiological conditions stabilized  
 290 the pH almost immediately after disruption (8.2 for replete and 8.0 for depleted). In  
 291 addition, the 5 g/L suspension of the N-replete culture had a stable and lower pH of 7.8  
 292 after 120 minutes. The N-depleted condition at the same concentration and in the same  
 293 period did not achieve stability (around pH 7.5). The same was observed for the highest  
 294 suspension concentrations (10 g/L) for both physiological conditions in the 180 minutes  
 295 test. These conditions tended to attain even lower pH values (around pH 7). This could  
 296 be explained by the fact that when 5 and 10 g/L cultures are milled, ions like  $H^+$  and  
 297 other organic compounds are released in proportion to cell concentration and stress level

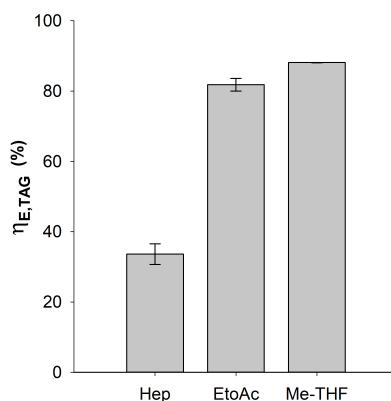


Figure 4: Triacylglycerol extraction efficiency for heptane (Hep), ethyl acetate (EtoAc) and 2-methyl-tetra-hydrofuran (Me-THF). Error bars for SE ( $n = 2$ )

298 (these compounds possibly being accumulated under stress conditions as a cell regulation  
 299 mechanism [44]). Presumably, the release of these ions and molecules, added to the rest  
 300 of the culture medium, could interact until the whole solution reaches an equilibrium.  
 301 The pH stabilization time would depend on the abundance of these molecules and their  
 302 interaction in the final mixture. It would therefore appear that the suspension needs to  
 303 be processed for the first 50 minutes after cell disruption, at most, to avoid any undesired  
 304 interaction, which could affect the recovery process.

### 305 3.3. Choice of Solvent for Extraction

306 Fig. 4 shows the extraction efficiency results for N-depleted biomass using the three  
 307 solvents tested. Me-THF and EtoAc showed a similar extraction efficiency  $\eta_{E,TAG}$ : up to  
 308 88% and 82% respectively. Heptane had the lowest at 34%. In all cases, TAG represented  
 309 89% of the measured TFA, showing that the solvents used have no relevant selectivity  
 310 for TAG.

311 In addition, by using cell destruction prior to extraction, the solvents (or mixtures)  
 312 did not depend on their ability to draw lipids from the cell (such as 2:1 v/v  $\text{CHCl}_3/\text{MeOH}$   
 313 [28]) but only on their affinity with lipid molecules, since TAG molecules were already re-  
 314 leased into the medium. This enabled maximization of extraction efficiency and thereby  
 315 reduction of the amount of solvent used, which would also significantly reduce the in-  
 316 vestment in solvent required for the whole wet extraction process.

317 As a result, Me-THF will be selected for future experiments as the best of the three  
318 solvents for recovering TAG.

#### 319 *3.4. Centrifugal Partition Extraction*

320 Centrifugal partition extraction (CPE) was used only as a reference to compare the  
321 specific solvent consumption ( $\Gamma_{Me-THF}$ ) of the optimal CCE results from the Box-  
322 Benhken RSM.

323 For a single TAG extraction carried out with a CPE device, it was possible to treat  
324 2 L at a biomass concentration 5 g/L with only 140 mL of solvent.

325 These values represent a TAG extraction efficiency  $\eta_{E,TAG}$  of 83% (SE = 3%, n = 3),  
326 which corresponds to a specific solvent consumption of  $\Gamma_{Me-THF}$  of 27.7 g<sub>Me-THF</sub>/g<sub>TAG</sub>.

#### 327 *3.5. Continuous Centrifugal Extraction*

328 The Box-Benhken RSM was chosen as the method for optimizing the main CCE  
329 parameters. The optimal value obtained with this method, added to the bead milling  
330 results, was expected to provide relevant information on the overall efficiency of the  
331 wet-extraction method in the biodiesel context.

332 Pre-tests were run prior to the main analysis to clarify the operating CCE work zone.  
333 Emulsions were readily obtained when the rotation speed of the CCE device exceeded  
334 certain limits. These limits varied for each observation unit (OU) but were within the  
335 5000 to 6000 rpm range (670 - 966 rcf). A relationship was observed between this rota-  
336 tional speed limit and the total supplied flow (ToT) for the different substances. Higher  
337 speeds promoted separation of the phases, but also the formation of emulsion. This phe-  
338 nomenon could be due to Taylor vortexes occurring during the centrifugal extraction and  
339 driving more complex variations in fluid dynamics when the rotation speed was increased  
340 [45, 46]. There is therefore a compromise between emulsification and separation when  
341 using a CCE module.

342 Another factor that could influence emulsification and therefore extraction efficiency  
343 ( $\eta_{E,i}$ ) is the release of intracellular material into the medium. It has been shown that  
344 some microalgae proteins have emulsifying properties [47]. Similarly, the cell debris  
345 could also form particle-stabilized emulsions known as Pickering emulsions [48]. Biomass  
346 concentration and disruption rate, therefore, also influence this phenomenon; for a given



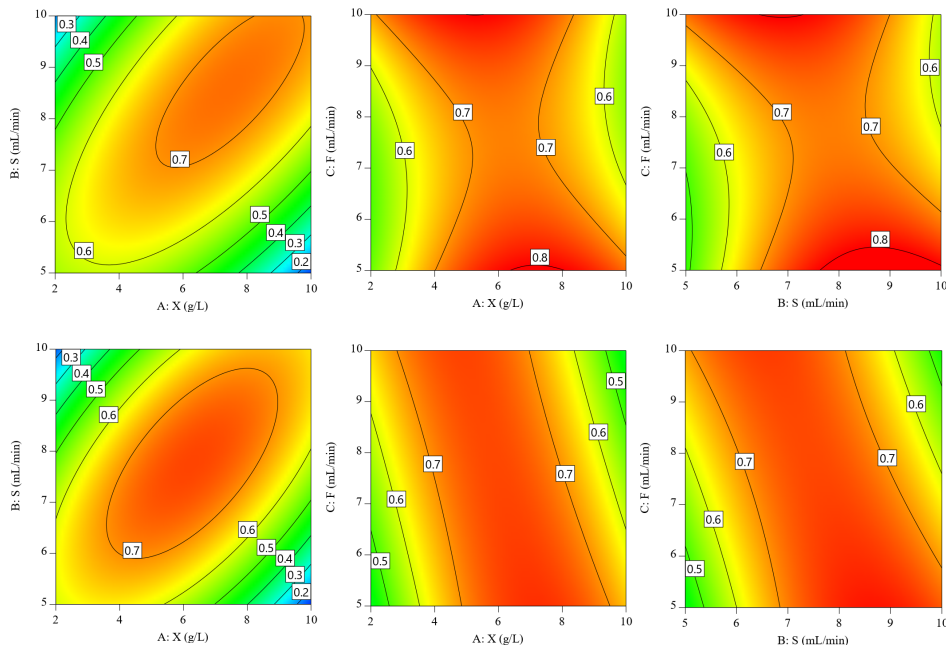


Figure 5: Contour graphs for each interaction between sources for the regression model obtained by Box-Behnken for extraction efficiency,  $\eta_{E,i}$  response. The contour lines represent extraction efficiency,  $\eta_{E,i}$  levels; a), b) and c) for **Total Fatty Acid (TFA)** and d), e) and f) for **Triacylglycerol (TAG)**.

347 high biomass suspension, increasing the disruption rate  $\tau_D$  will also release emulsifying  
 348 molecules/particles. Accordingly, additional pre-tests were run to clarify the biomass  
 349 concentration range to avoid emulsification as far as possible. Normally, cultures above  
 350 10 g/L are unmanageable for extraction due to the immediate appearance of an emulsion,  
 351 even when working at low  $S/F$  ratios or low rotation speeds ( $< 4000$  rpm / 429 rcf). For  
 352 example, when working with suspensions above 10 g/L of biomass, emulsions appeared  
 353 from 3500 rpm (329 rcf). A higher rotation speed was therefore required for recovering  
 354 the same outlet flow rates (since  $ToT = S + F = E + R$ ), although no solvent was  
 355 recovered, just an enhanced emulsion. These pre-tests defined the operational range  
 356 of biomass concentration as between 2-10 g/L for RSM analysis. Protein content and  
 357 operational pH were not considered as variables for RSM.

358 The RSM experimental results are detailed in Appendix A, Table A.3. The resulting  
 359 contour graphics (Fig. 5) describing the extraction efficiency as a response of the oper-

360 ational variables may therefore be useful for navigating within the limits of the CCE.  
361 Using the biomass - solvent interaction ( $X - S$ ), as a first reference, Figs. 5a and 5d show  
362 the maximal extraction efficiency  $\eta_{E,i}$  as being within  $S$ : 7-10 mL/min and  $X$ : 5-10 g/L.  
363 This zone can therefore be transposed to the  $X-F$  and  $S-F$  interactions (Figs. 5b, 5c,  
364 5e, 5f) where higher efficiencies are found at a low feed rate.

365 The numerical results obtained (see Appendix A) provide a tool for locating the  
366 optimal point for the three simultaneous sources. It was found that  $\eta_{E,TFA} = 0.93$  at  $X$   
367 = 8.3 g/L,  $S = 9.2$  mL/min,  $F = 5.0$  mL/min and  $\eta_{E,TAG} = 0.84$  at  $X = 7.9$  g/L,  $S = 8.9$   
368 mL/min and,  $F = 5.4$  mL/min. Both efficiency points were consistent with the previous  
369 analyses. The values obtained were higher than with the  $CHCl_3$ /methanol wet extraction  
370 (extraction efficiency,  $\eta_{E,i} = 50\%$ ) carried out by Angles et al. [9]. Remember, however,  
371 that the values correspond to the 80% of lipids released in the bead milling operation.

372 With the optimal point obtained by the experiment design, the specific solvent con-  
373 sumption for CCE was determined as  $\Gamma_{Me-THF} = 213.8$  g<sub>Me-THF</sub>/g<sub>TAG</sub>.

374 Note that  $\Gamma_{Me-THF}$  is linked to the energy consumption for the whole biodiesel  
375 process, since more energy is required for distilling each gram of solvent used to produce  
376 each liter of biodiesel. These values show that if scaled up, CPE technology could save 7.8  
377 times more solvent than CCE, even though the two technologies have similar extraction  
378 efficiencies.

379 However, the results for CCE could be improved. On the one hand, this work has  
380 demonstrated the relationship between stress levels, biomass concentration and the re-  
381 lease of intracellular material with the formation of emulsion, and has revealed the work  
382 zone to be avoided when carrying out CCE. In this regard, more research on the optimiza-  
383 tion of hydrodynamics in the CCE chamber could enable working with higher biomass  
384 concentrations, which would increase recovery. On the other hand, CCE efficiency can  
385 also be improved by using several devices connected in series (the present work relating  
386 to a single module). This approach is also valuable in terms of the scalability of the  
387 operation, which is one of the biggest advantages of CCE over CPE.

388 As stated, many factors other than those relating to the appearance of emulsification  
389 (such as pH and temperature) that were not studied in detail in the present work, in-  
390 teract during centrifugal extraction and should be investigated for future experiments in

391 biodiesel production.

392 The optimal wet extraction yield of 73% obtained with bead milling combined with  
393 CCE (using Me-THF) has been demonstrated as a high-performance TAG recovery tech-  
394 nique with the advantage of scalability for the biodiesel process. The process may perform  
395 better than extraction yields in the literature. For example, different solvent mixtures  
396 and cell disruptions for *N. gaditana* were tested by Ryckeboosch et al. [49], where solvents  
397 such as hexane/isopropanol, ethyl acetate/hexane and ethanol were found to be the best  
398 of six, with extraction yields of 58%, 46% and 52% respectively. Similarly, Sati et al.  
399 [50] reviewed extraction yields from other pre-extraction treatments such as mechanical  
400 (35%), surfactant (78%) and enzymatic lysis (73%). There are other techniques effective  
401 for biodiesel application too, such as the simultaneous distillation and extraction process,  
402 which gave a 24% extraction yield with *N. oculata* [51], and microwave combined with  
403 super-critical CO<sub>2</sub> extraction, which achieved a 30% extraction yield with *N. salina* [52].

#### 404 **4. Conclusion**

405 Wet extraction operations (bead milling combined with centrifugal extraction) achieved  
406 a final TAG recovery of 73% using CCE technology with *Nannochloropsis gaditana* cul-  
407 tivated in N-depleted media. Physiological variables such as cell fragility, and process  
408 operating conditions such as harvesting concentration, were found to affect the whole  
409 process. The key variables and their interactions during lipid recovery were determined  
410 and optimized by RSM analysis. However, CCE uses around eight times more solvent  
411 than CPE. Consequently, **further intensification of the extraction step** is required to  
412 combine scalability (*i.e.* the CCE process) with a reduction in solvent consumption and  
413 emulsification issues for biodiesel production.

#### 414 **Acknowledgements**

415 VH acknowledges the National Science and Technology Council (CONACyT, Mexico)  
416 for his research fellowship. All the authors acknowledge the contributions made by B.  
417 Le Gouic, J. Tallec, S. Chollet, L. Herve and M. Cueff

418 Funding: This research did not receive any specific grant from funding agencies in  
419 the public, commercial, or not-for-profit sectors.

420 **CRedit authorship contribution statement**

421 Vladimir Heredia: Conceptualization, Formal analysis, Investigation, Writing - Original  
422 Draft. Jeremy Pruvost: Writing - Review & Editing, Supervision. Olivier Gonçalves:  
423 Writing - Review & Editing. Luc Marchal: Conceptualization, Investigation, Writing -  
424 Review & Editing, Supervision.

425 **Informed Consent, Human/Animal Rights Statement**

426 No conflicts, informed consent, or human or animal rights are applicable to this study.

427 **References**

- 428 [1] Y. Chisti, Biodiesel from microalgae, *Biotechnology Advances* 25 (2007) 294–306.
- 429 [2] T. A. Beacham, C. Bradley, D. A. White, P. Bond, S. T. Ali, Lipid productivity and cell wall  
430 ultrastructure of six strains of *Nannochloropsis*: Implications for biofuel production and downstream  
431 processing, *Algal Research* 6 (2014) 64–69.
- 432 [3] X. Ma, J. Liu, B. Liu, T. Chen, B. Yang, F. Chen, Physiological and biochemical changes reveal  
433 stress-associated photosynthetic carbon partitioning into triacylglycerol in the oleaginous marine  
434 alga *Nannochloropsis oculata*, *Algal Research* 16 (2016) 28–35.
- 435 [4] Y. Ma, Z. Wang, C. Yu, Y. Yin, G. Zhou, Evaluation of the potential of 9 *Nannochloropsis* strains  
436 for biodiesel production, *Bioresource Technology* 167 (2014) 503–509.
- 437 [5] D. Bouillaud, V. Heredia, T. Castaing-Cordier, D. Drouin, B. Charrier, O. Gonçalves, J. Farjon,  
438 P. Giraudeau, Benchtop flow NMR spectroscopy as an online device for the in vivo monitoring of  
439 lipid accumulation in microalgae, *Algal Research* 43 (2019) 101624.
- 440 [6] A. Taleb, J. Pruvost, J. Legrand, H. Marec, B. Le-Gouic, B. Mirabella, B. Legeret, S. Bouvet,  
441 G. Peltier, Y. Li-Beisson, S. Taha, H. Takache, Development and validation of a screening proce-  
442 dure of microalgae for biodiesel production: Application to the genus of marine microalgae *Nan-*  
443 *nochloropsis*, *Bioresource Technology* 177 (2015) 224–232.
- 444 [7] K. J. Flynn, K. Davidson, A. Cunningham, Relations between carbon and nitrogen during growth  
445 of *Nannochloropsis oculata* (Droop) Hibberd under continuous illumination, *New Phytologist* 125  
446 (1993) 717–722.
- 447 [8] J. Camacho-Rodríguez, A. M. González-Céspedes, M. C. Cerón-García, J. M. Fernández-Sevilla,  
448 F. G. Ación-Fernández, E. Molina-Grima, A quantitative study of eicosapentaenoic acid (EPA)  
449 production by *Nannochloropsis gaditana* for aquaculture as a function of dilution rate, temperature  
450 and average irradiance, *Applied Microbiology and Biotechnology* 98 (2014) 2429–2440.
- 451 [9] E. Angles, P. Jaouen, J. Pruvost, L. Marchal, Wet lipid extraction from the microalga *Nan-*  
452 *nochloropsis* sp.: Disruption, physiological effects and solvent screening, *Algal Research* 21 (2017)  
453 27–34.
- 454 [10] J. H. Janssen, P. P. Lamers, R. C. de Vos, R. H. Wijffels, M. J. Barbosa, Translocation and de novo  
455 synthesis of eicosapentaenoic acid (EPA) during nitrogen starvation in *Nannochloropsis gaditana*,  
456 *Algal Research* 37 (2019) 138–144.
- 457 [11] V. Montalescot, T. Rinaldi, R. Touchard, S. Jubeau, M. Frappart, P. Jaouen, P. Bourseau, L. Mar-  
458 chal, Optimization of bead milling parameters for the cell disruption of microalgae: Process mod-  
459 eling and application to *Porphyridium cruentum* and *Nannochloropsis oculata*, *Bioresource Tech-*  
460 *nology* 196 (2015) 339–346.
- 461 [12] M. J. Scholz, T. L. Weiss, R. E. Jinkerson, J. Jing, R. Roth, U. Goodenough, M. C. Posewitz, H. G.  
462 Gerken, Ultrastructure and composition of the *Nannochloropsis gaditana* cell wall, *Eukaryotic Cell*  
463 13 (2014) 1450–1464.
- 464 [13] X. B. Tan, M. K. Lam, Y. Uemura, J. W. Lim, C. Y. Wong, K. T. Lee, Cultivation of microalgae

- 465 for biodiesel production: A review on upstream and downstream processing, *Chinese Journal of*  
466 *Chemical Engineering* 26 (2018) 17–30.
- 467 [14] M. Axelsson, F. Gentili, A single-step method for rapid extraction of total lipids from green  
468 microalgae, *PLoS ONE* 9 (2014) 17–20.
- 469 [15] S. A. Scott, M. P. Davey, J. S. Dennis, I. Horst, C. J. Howe, D. J. Lea-Smith, A. G. Smith, Biodiesel  
470 from algae: Challenges and prospects, *Current Opinion in Biotechnology* 21 (2010) 277–286.
- 471 [16] R. Halim, R. Harun, M. K. Danquah, P. A. Webley, Microalgal cell disruption for biofuel develop-  
472 ment, *Applied Energy* 91 (2012) 116–121.
- 473 [17] H. Taher, S. Al-Zuhair, A. H. Al-Marzouqi, Y. Haik, M. Farid, Effective extraction of microalgae  
474 lipids from wet biomass for biodiesel production, *Biomass and Bioenergy* 66 (2014) 159–167.
- 475 [18] T. Dong, E. P. Knoshaug, P. T. Pienkos, L. M. Laurens, Lipid recovery from wet oleaginous  
476 microbial biomass for biofuel production: A critical review, *Applied Energy* 177 (2016) 879–895.
- 477 [19] A. K. Lee, D. M. Lewis, P. J. Ashman, Disruption of microalgal cells for the extraction of lipids  
478 for biofuels: Processes and specific energy requirements, *Biomass and Bioenergy* 46 (2012) 89–101.
- 479 [20] F. Ghasemi Naghdi, L. M. González González, W. Chan, P. M. Schenk, Progress on lipid extraction  
480 from wet algal biomass for biodiesel production, *Microbial Biotechnology* 9 (2016) 718–726.
- 481 [21] R. Halim, B. Gladman, M. K. Danquah, P. A. Webley, Oil extraction from microalgae for biodiesel  
482 production, *Bioresource Technology* 102 (2011) 178–185.
- 483 [22] H. M. Amaro, A. C. Guedes, F. X. Malcata, Advances and perspectives in using microalgae to  
484 produce biodiesel, *Applied Energy* 88 (2011) 3402–3410.
- 485 [23] J. Y. Lee, C. Yoo, S. Y. Jun, C. Y. Ahn, H. M. Oh, Comparison of several methods for effective  
486 lipid extraction from microalgae, *Bioresource Technology* 101 (2010) S75–S77.
- 487 [24] J. Kim, G. Yoo, H. Lee, J. Lim, K. Kim, C. W. Kim, M. S. Park, J. W. Yang, Methods of  
488 downstream processing for the production of biodiesel from microalgae, *Biotechnology Advances*  
489 31 (2013) 862–876.
- 490 [25] T. R. Zinkoné, I. Gifuni, L. Lavenant, J. Pruvost, L. Marchal, Bead milling disruption kinetics of  
491 microalgae: Process modeling, optimization and application to biomolecules recovery from *Chlorella*  
492 *sorokiniana*, *Bioresource Technology* 267 (2018) 458–465.
- 493 [26] C. Safi, C. Frances, A. V. Ursu, C. Laroche, C. Pouzet, C. Vaca-Garcia, P. Y. Pontalier, Under-  
494 standing the effect of cell disruption methods on the diffusion of *Chlorella vulgaris* proteins and  
495 pigments in the aqueous phase, *Algal Research* 8 (2015) 61–68.
- 496 [27] J. Folch, M. Lees, G. Sloane Stanley, A simple method for the isolation and purification of total  
497 lipides from animal tissues 55 (1987) 999–1033.
- 498 [28] E. G. Bligh, W. J. Dyer, A Rapid Method Of Total Lipid Extraction And Purification, *Canadian*  
499 *Journal of Biochemistry and Physiology* 37 (1959) 911–917.
- 500 [29] P. Li, K. Sakuragi, H. Makino, Extraction techniques in sustainable biofuel production: A concise  
501 review, *Fuel Processing Technology* 193 (2019) 295–303.
- 502 [30] P. Watts, Chloroform, Technical Report 58, World Health Organization, Geneva, Switzerland, 2004.  
503 URL: <https://www.who.int/ipcs/publications/cicad/en/>.

- 504 [31] D. Reay, C. Ramshaw, A. Harvey (Eds.), *Process Intensification*, Elsevier, 2008. doi:10.1016/  
505 B978-0-7506-8941-0.X0001-6.
- 506 [32] B. Seyfang, A. Klein, T. Grützner, *Extraction Centrifuges—Intensified Equipment Facilitating*  
507 *Modular and Flexible Plant Concepts*, *ChemEngineering* 3 (2019) 17.
- 508 [33] M. Bojczuk, D. Żyżelewicz, P. Hodurek, *Centrifugal partition chromatography – A review of recent*  
509 *applications and some classic references*, *Journal of Separation Science* 40 (2017) 1597–1609.
- 510 [34] K. Schügerl, *Solvent Extraction in Biotechnology*, volume 8, Springer Berlin Heidelberg, Berlin,  
511 Heidelberg, 1994. doi:10.1007/978-3-662-03064-6.
- 512 [35] C. Ungureanu, L. Marchal, A. A. Chirvase, A. Foucalt, *Centrifugal partition extraction, a new*  
513 *method for direct metabolites recovery from culture broth: Case study of torularhodin recovery*  
514 *from Rhodotorula rubra*, *Bioresource Technology* 132 (2013) 406–409.
- 515 [36] J. A. Berges, D. J. Franklin, P. J. Harrison, *Evolution of an artificial seawater medium: Improve-*  
516 *ments in enriched seawater, artificial water over the last two decades*, *Journal of Phycology* 37  
517 (2001) 1138–1145.
- 518 [37] J. Pruvost, G. Van Vooren, B. Le Gouic, A. Couzinet-Mossion, J. Legrand, *Systematic investiga-*  
519 *tion of biomass and lipid productivity by microalgae in photobioreactors for biodiesel application*,  
520 *Bioresource Technology* 102 (2011) 150–158.
- 521 [38] B. Moutel, O. Gonçalves, F. Le Grand, M. Long, P. Soudant, J. Legrand, D. Grizeau, J. Pruvost,  
522 *Development of a screening procedure for the characterization of Botryococcus braunii strains for*  
523 *biofuel application*, *Process Biochemistry* 51 (2016) 1855–1865.
- 524 [39] S. Kim, J. Chen, T. Cheng, A. Gindulyte, J. He, S. He, Q. Li, B. A. Shoemaker, P. A. Thiessen,  
525 B. Yu, L. Zaslavsky, J. Zhang, E. E. Bolton, *PubChem 2019 update: improved access to chemical*  
526 *data*, *Nucleic Acids Research* 47 (2019) D1102–D1109.
- 527 [40] A.-G. Sicaire, M. A. Vian, A. Filly, Y. Li, A. Bily, F. Chemat, *2-Methyltetrahydrofuran: Main*  
528 *Properties, Production Processes, and Application in Extraction of Natural Products*, 2014, pp.  
529 253–268. doi:10.1007/978-3-662-43628-8\_12.
- 530 [41] L. Marchal, J. Legrand, A. Foucalt, *Mass transport and flow regimes in centrifuga partition*  
531 *chromatography*, *AIChE Journal* 48 (2002) 1692–1704.
- 532 [42] L. Marchal, M. Mojaat-Guemir, A. Foucalt, J. Pruvost, *Centrifugal partition extraction of  $\beta$ -*  
533 *carotene from Dunaliella salina for efficient and biocompatible recovery of metabolites*, *Bioresource*  
534 *Technology* 134 (2013) 396–400.
- 535 [43] M. R. Heath, K. Richardson, T. Kirboe, *Optical assessment of phytoplankton nutrient depletion*,  
536 *Journal of Plankton Research* 12 (1990) 381–396.
- 537 [44] M. A. Borowitzka, *The ‘stress’ concept in microalgal biology—homeostasis, acclimation and adap-*  
538 *tation*, *Journal of Applied Phycology* 30 (2018) 2815–2825.
- 539 [45] J. T. Stuart, *Taylor-Vortex Flow: A Dynamical System*, *SIAM Review* 28 (1986) 315–342.
- 540 [46] M. Nakase, K. Takeshita, *Numerical and Experimental Study on Oil-water Dispersion in New*  
541 *Countercurrent Centrifugal Extractor*, *Procedia Chemistry* 7 (2012) 288–294.
- 542 [47] S. Ebert, L. Grossmann, J. Hinrichs, J. Weiss, *Emulsifying properties of water-soluble proteins*



- 543 extracted from the microalgae: *Chlorella sorokiniana* and *Phaeodactylum tricornutum*, *Food and*  
544 *Function* 10 (2019) 754–764.
- 545 [48] H. Jiang, Y. Sheng, T. Ngai, Pickering emulsions: Versatility of colloidal particles and recent  
546 applications, *Current Opinion in Colloid & Interface Science* 49 (2020) 1–15.
- 547 [49] E. Ryckeboosch, S. P. C. Bermúdez, R. Termote-Verhalle, C. Bruneel, K. Muylaert, R. Parra-  
548 Saldívar, I. Foubert, Influence of extraction solvent system on the extractability of lipid components  
549 from the biomass of *Nannochloropsis gaditana*, *Journal of Applied Phycology* 26 (2014) 1501–1510.
- 550 [50] H. Sati, M. Mitra, S. Mishra, P. Baredar, Microalgal lipid extraction strategies for biodiesel pro-  
551 duction: A review, *Algal Research* 38 (2019) 101413.
- 552 [51] C. Dejoye Tanzi, M. Abert Vian, F. Chemat, New procedure for extraction of algal lipids from wet  
553 biomass: A green clean and scalable process, *Bioresource Technology* 134 (2013) 271–275.
- 554 [52] P. D. Patil, K. P. R. Dandamudi, J. Wang, Q. Deng, S. Deng, Extraction of bio-oils from algae  
555 with supercritical carbon dioxide and co-solvents, *Journal of Supercritical Fluids* 135 (2018) 60–68.
- 556 [53] G. E. P. Box, D. W. Behnken, Some New Three Level Designs for the Study of Quantitative  
557 Variables, *Technometrics* 2 (1960) 455.
- 558 [54] S. L. Ferreira, R. E. Bruns, H. S. Ferreira, G. D. Matos, J. M. David, G. C. Brandão, E. G. da Silva,  
559 L. A. Portugal, P. S. dos Reis, A. S. Souza, W. N. dos Santos, Box-Behnken design: An alternative  
560 for the optimization of analytical methods, *Analytica Chimica Acta* 597 (2007) 179–186.

## 561 **Appendix A. CCE operating parameter optimization: RSM approach**

### 562 *A.1. Introduction*

563 The Box-Behnken response surface methodology (RSM) was designed [53, 54] to  
564 clarify the interaction between operating parameters in the CCE wet extractor. Contrary  
565 to the usual factorial RSM (where variables are arranged in an n-dimensional space and  
566 all combinations are considered for the experiment setup), the Box-Behnken RSM is  
567 arranged as a spherical set of variables, which means that the number of experiment runs  
568 is reduced and the extreme interaction vertices are not considered. It is advantageous  
569 because certain combinations of factors (in this work and others) could be physically  
570 restrictive or expensive to operate.

571 Using this RSM, a response surface is obtained that can be modeled and analyzed  
572 using the ANOVA method, which looks for the greatest interaction impacting the re-  
573 sponse.

### 574 *A.2. experiment setup*

575 The Box-Behnken RSM included 15 observation units (OUs) for three independent  
576 factors and one response variable: 12 OUs derived from independent variables around 3  
577 other OUs as replicates of the central point. Ranges and variables were biomass concen-  
578 tration (from bead milling)  $X = 2, 5, 10$  g/L and solvent and feed inlets  $S$  and  $F = 5,$   
579  $7.5, 10$  mL/min each. The results of experiments carried out with all the observations  
580 units performed are presented in Table A.3.

581 The TFA/TAG extraction efficiency ( $\eta_{E,i}$ ) results from the 15 OUs were processed  
582 using Design Expert V11 (Stat-Ease, US). For some analyses, the variables were coded  
583 as follows:  $X$  as A,  $S$  as B and  $F$  as C. The software provided random experimental  
584 design, statistical analysis and numerical and graphical optimization.

### 585 *A.3. RSM data analysis*

586 After running the Design Expert software, the data were found to fit well with a  
587 quadratic-order model. Fig. A.1 shows that with the experiment extraction efficiency  
588  $\eta_{E,i}$ , which corresponds with a high biomass concentration,  $X$  and  $S$  cannot actually  
589 be fitted into a model because of the sudden increase (mainly due to the unexpected  
590 appearance of emulsion at these values).

Table A.3: Experimental results obtained by the Box-Benhken RSM analysis for the **Total Fatty Acid** ( $\eta_{E,TFA}$ ) and Triacylglycerol ( $\eta_{E,TAG}$ ) extraction efficiencies. OU - observation unit; A, B and C are the coded values for **biomass concentration (X), solvent inlet rate (S) and feed inlet rate (F)** respectively.

O.U.	A : X (g/L)	B : S (mL/min)	C : F (mL/min)	$\eta_{E,TFA}$	$\eta_{E,TAG}$
1	2,0	7,5	10,0	84%	81%
2	2,0	7,5	5,0	55%	48%
3	2,0	5,0	7,5	42%	41%
4	2,0	10,0	7,5	15%	13%
5	5,0	10,0	5,0	73%	62%
6	5,0	7,5	7,5	70%	74%
7	5,0	7,5	7,5	70%	74%
8	5,0	10,0	10,0	44%	30%
9	5,0	5,0	10,0	78%	79%
10	5,0	5,0	5,0	59%	56%
11	5,0	7,5	7,5	70%	73%
12	10,0	10,0	7,5	82%	80%
13	10,0	7,5	10,0	51%	34%
14	10,0	7,5	5,0	60%	52%
15	10,0	5,0	7,5	21%	19%

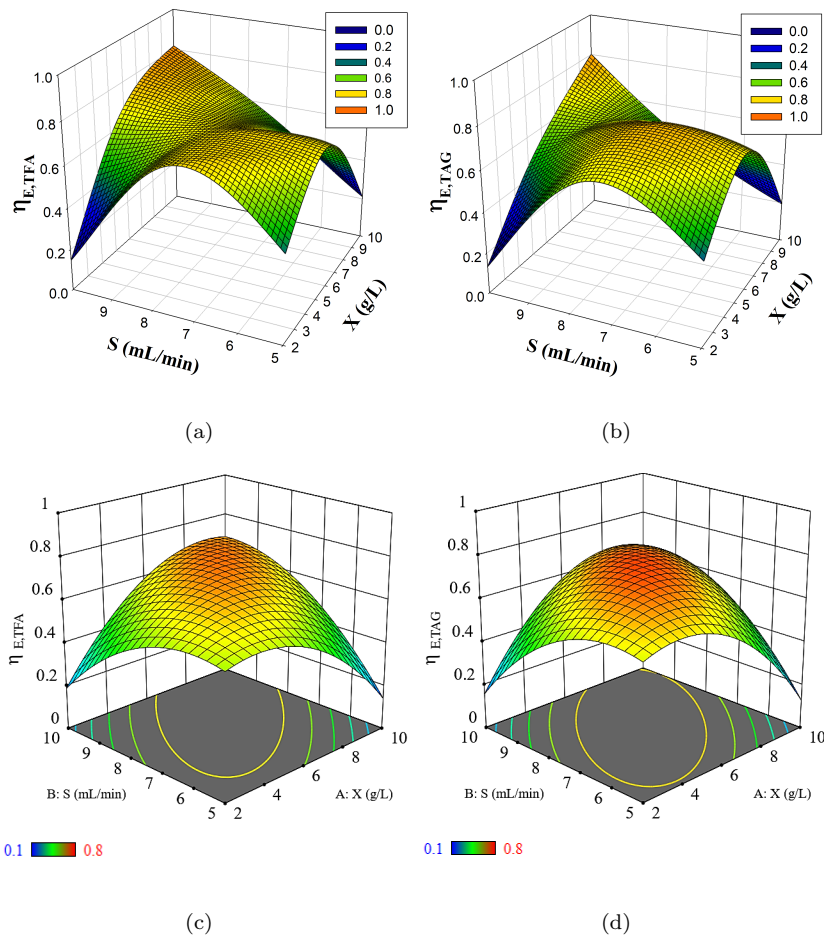


Figure A.1: Raw experiment data and quadratic 3D mesh model for the influence of solvent-to-biomass concentration on extraction efficiency,  $\eta_{E,i}$ . a) and b) unprocessed data for Total Fatty Acid (TFA) and Triacylglycerol (TAG) respectively. c) and d) data obtained after modeling

Table A.4: Analysis of variance (ANOVA) for modeling of a quadratic order. Values for surface response on **Total Fatty Acid (TFA) and Triacylglycerol (TAG)** extraction efficiency are shown.

Source	AGT					TAG				
	SS	df	Mean Square	F-value	p-value	SS	df	Mean Square	F-value	p-value
<i>Model</i>	0.4980	9	0.0553	2.730	0.141	0.5790	9	0.0643	2.150	0.207
<i>A-Biomass conc.</i>	0.0033	1	0.0033	0.164	0.702	0.0001	1	0.0001	0.003	0.962
<i>B-Solvent</i>	0.0156	1	0.0156	0.770	0.420	0.0026	1	0.0026	0.088	0.779
<i>C-Feed</i>	0.0001	1	0.0001	0.001	0.977	0.0003	1	0.0003	0.010	0.925
<i>AB</i>	0.2179	1	0.2179	10.740	0.022	0.2303	1	0.2303	7.700	0.039
<i>AC</i>	0.0279	1	0.0279	1.380	0.294	0.0557	1	0.0557	1.860	0.231
<i>BC</i>	0.0553	1	0.0553	2.730	0.160	0.0727	1	0.0727	2.430	0.180
<i>A<sup>2</sup></i>	0.0892	1	0.0892	4.400	0.090	0.1307	1	0.1307	4.370	0.091
<i>B<sup>2</sup></i>	0.0765	1	0.0765	3.770	0.110	0.1006	1	0.1006	3.360	0.126
<i>C<sup>2</sup></i>	0.0246	1	0.0246	1.210	0.321	0.0002	1	0.0002	0.007	0.937
<i>Std.Dev.</i>	0.142					0.173				
<i>Mean</i>	0.582					0.546				
<i>C.V.%</i>	24.482					31.700				
<i>R<sup>2</sup></i>	0.831					0.795				

591 The analysis of variance (Table A.4) showed that first-order sources (A, B and C)  
592 seem to have less significance than second-order sources (AB, AC, BC, A<sup>2</sup>, B<sup>2</sup> and C<sup>2</sup>).  
593 On the whole, interactions and additives affected the model response more than isolated  
594 variables: AB and A<sup>2</sup> are the only ones below  $\alpha = 0.1$ . The same trends were obtained  
595 for TFA and TAG.

596 The results reported in the section 3.5 for maximum extraction efficiency in the model  
597 were obtained using  $\alpha = 0.05$  in the numerical solution provided by the Design Expert  
598 software.

599 The estimated coefficients are shown in table A.5. These represent the expected  
600 shift in response per unit factor value, with the other factors constant. To obtain these  
601 coefficients using the Box-Benhken RSM, the source values had to be coded as +1 for  
602 the higher levels and -1 for the lower ones. This type of analysis enabled identification of  
603 the relative impact of the factors by comparing their coefficients. The equation produced  
604 with these coefficients could be used to predict the effects in the response, but only within  
605 the coded limits of each source.

606 By ignoring the additive variables, for example, the source AB (Coeff<sub>TFA</sub>: 0.230,  
607 Coeff<sub>TAG</sub>: 0.236) was shown to have the greatest proportional effect on extraction effi-

Table A.5: Estimated regression coefficients in terms of coded factors and final equation coefficients in terms of actual factors, both obtained from the quadratic model obtained for **Total Fatty Acid (TFA)** and **Triacylglycerol (TAG)** wet-extraction efficiency.

Factor	TFA		TAG	
	Coefficient estimate	Final equation coefficient	Coefficient estimate	Final equation coefficient
<i>Intercept</i>	0.712	-0.792	0.753	-1.973
<i>A- Biomass conc.</i>	0.020	0.0206	0.003	0.0634
<i>B-Solvent</i>	0.045	0.3667	0.018	0.4235
<i>C-Feed</i>	0.002	-0.005	-0.006	0.247
<i>AB</i>	0.230	0.023	0.236	0.0236
<i>AC</i>	-0.082	-0.008	-0.116	-0.012
<i>BC</i>	-0.118	-0.019	-0.135	-0.022
<i>A<sup>2</sup></i>	-0.168	-0.011	-0.204	-0.013
<i>B<sup>2</sup></i>	-0.144	-0.023	-0.165	-0.026
<i>C<sup>2</sup></i>	0.082	0.0131	-0.008	-0.001

608 ciency  $\eta_{E,i}$ , followed by an inverse-proportional effect on the relationship between  $S$  and  
609  $F$  (Coeff<sub>TFA</sub>: -0.118, Coeff<sub>TAG</sub>: -0.135). This simply means that if more lipids are to be  
610 recovered, a higher  $S$  should also be used, but the effect is diminished if  $F$  is increased  
611 in relation to  $S$ . A high concentration would require more time and interface contact  
612 with the solvent, which can be achieved by reducing the feed rate for CCE. On the other  
613 hand, the effect of the additive variables is also highest for  $A^2$  and  $B^2$ . Table A.5 also  
614 shows the coefficients for the equation in terms of actual factors. This could be used  
615 to predict the extraction efficiency  $\eta_{E,i}$  for given levels of each factor. Here, the levels  
616 should be specified in the original units for each factor.

617 Nevertheless, neither type of coefficient obtained for regression in this work can be  
618 used to accurately predict extraction efficiency  $\eta_{E,i}$  precisely, due to the low  $R^2$  and  
619 moderate p-value of the model itself. However,  $R^2$  (0.831 for TFA and 0.795 for TAG)  
620 indicates only a reasonable correlation between the experimental and predicted values of  
621 the response. Despite this, the model still provides important information on the rela-  
622 tionship between the parameters, which is clearer when the contour graphs are analyzed.

623 Note that the reason for using Box-Behnken RSM for this work was to determine the  
624 general extraction trend as a function of the main operating parameters (such as biomass  
625 concentration and solvent and biomass flow rates) and also to determine an operational  
626 CCE work-zone.